Design Study on Mixing Performance of Rotational Vanes in Subchannel with Fuel Rod Bundles

Han Eol Park, In Cheol Bang*
Department of Nuclear Engineering, Ulsan National Institute of Science and Technology (UNIST),
50 UNIST-gil, Ulju-gun, Ulsan, 44919
**Corresponding author: icbang@unist.ac.kr*

1. Introduction

Mixing vane structure provides secondary flow such as swirl and cross flow that increases mixing and turbulence in the subchannel. It is important to predict and enhance secondary flow that influences lateral velocity, turbulence intensity, Reynolds stress, and pressure drop of fuel assembly.

To increase swirl flow, innovative mixing vane; rotational mixing vane was suggested and its performance in single channel was evaluated [1]. In addition to previous study, impeller-like rotational mixing vane is suggested, which adopts rotational turbine shape as open impeller structure.

Focused on the swirl generation from mixing vanes, CFD analysis was performed for 2×3 subchannel equipped various types of mixing vane; (1) spacer grid without vane (NV), (2) split vane (SV), and (3) rotational vane (RV). FLOW-3D is chosen to simulate above design candidates of rotational moving vane, which is capable to simulate fluid-induced rotation with general moving object (GMO).

2. CFD Modeling

2.1 Vane design

Fig. 1 shows the geometry of the NV, SV, RV and IV used in CFD simulation. NV is wall with 3 mm thickness, with 100 mm length, which acts as a base structure of all types of vane. The SV is depicted as 45° angle relative to the flow direction, 20 mm and 16 mm width is applied. The RV model has four blades, same angle with SV. Length of blade is 6 mm with height is also 6 mm, and thickness is 0.6 mm for the vane blades. IV has 16 blades to maximize secondary flow effect, has same length and height with RV.

2.2 Test section of subchannel

Test section is designed with rectangular subchannel, with 2×3 fuel rod. Scaling is considered to maximize visualization and evaluate the swirling effect of mixing vane in fuel assembly subchannel [4]. The section is 2.5 times scaled with typical Plus-7 fuel assembly channel. Bulk flow velocity ranges 0.28 m/s ~ 0.94 m/s, as Reynolds number of 4870 ~ 16340. For CFD model, 0.5 m/s vertical flow were dealt for the channel.

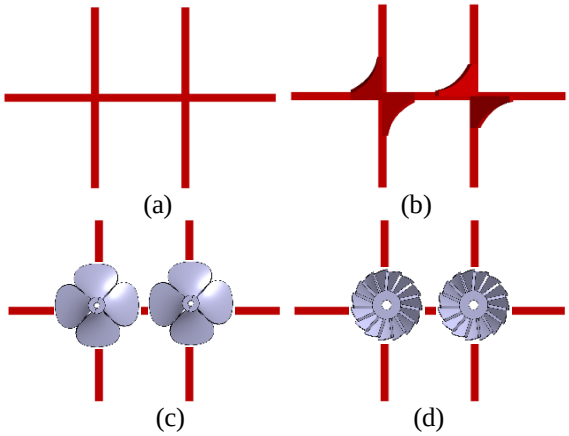

Fig. 1. Geometry of (a) NV, (b) SV, (c) RV (d) IV

2.3 Physics setup for FLOW-3D analysis

Several commercial CFD codes provide propeller models, but only prescribed rotating propeller is designed in CFD. GMO model in FLOW-3D serves General Moving Object (GMO) model, which can describe coupled motion of RV and IV with fluid flow. GMO is a rigid body under physical motion which is either dynamically coupled with fluid flow. Rotate about a fixed z-axis motion was set for the rotating mixing vane. GMO components can be of a mixed motion type, namely have translational and/or rotational velocities that are coupled in some coordinate directions and prescribed in the other directions. Therefore FLOW-3D is utilized to model mixing vane model in fluid flow.

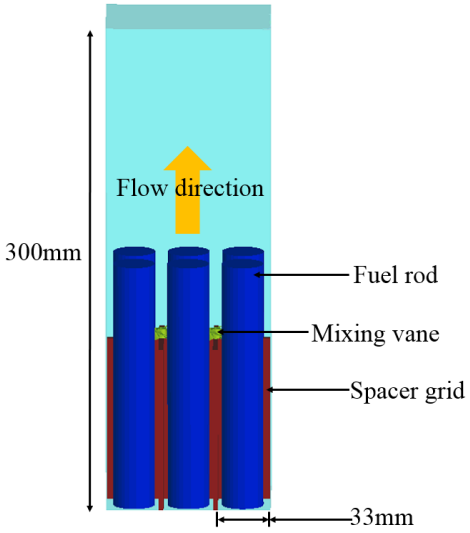

Fig. 2. CFD test section structure

k-ω turbulence model was used for modeling of inhomogeneous turbulent flow. The relative outlet pressure was 0 Pa to calculate the pressure drop.

For the analysis of moving object, volume of fluid (VOF) transport equation is used through flow-3D. The fluid volume and area work as source term for motion of moving object. The hydraulic force and torque due to pressure and shear stress are add in coupled motion, so equations of motion are solved for the moving objects under coupled motion. The moving object is updated each time step, based on the applied force based on the continuity equation and the VOF transport equation:

$$\frac{V_f}{\rho}\frac{\partial \rho}{\partial t}+\frac{1}{\rho}\nabla\bullet(\rho\vec{u}A_f)=\frac{-V_f}{\partial t} \quad (1)$$

$$\frac{\partial F}{\partial t}+\frac{1}{V_f}\nabla\bullet(F\vec{u}A_f)=-\frac{F}{V_f}\frac{\partial V_f}{\partial t} \quad (2)$$

, where V_f is the volume fraction, ρ is the fluid density, t is the time, $\vec{u}$ is the fluid velocity, A_f is the area fraction, and F is the fluid fraction [5]. Instead of RV, general gravity and non-inertial reference frame motion is solved with viscosity and turbulence model.

3. Results and Discussion

Figure 3 shows lateral velocity field at axial position of Z/D_h = 1, 2, 3 from the vane edge. SV shows drastic mixing effect beside the fuel rod. SV shows high lateral swirl but swirling area is highly dependent on the vane region. RV and IV generates swirl flow for lateral velocity, comparing to SV has relatively small but swirling is occurring evenly along with large area of subchannel.

The maximum lateral velocity was respectively high in SV, the decay of lateral velocity was high along with the z-axis development. The swirl decay is measured by the lateral velocity driven through the z-axis. Comparison to Z/D_h = 1, lateral velocity loss is represented as decay. SV has maximum lateral velocity of 0.138 m/s at Z/D_h = 1 position. However, RV and IV show less lateral velocity difference along with the axial position, with less maximum lateral velocity each 0.66, 0.47 for RV and IV respectively. At Z/D_h=1 to 3, swirl decay was relatively low along with the z-axis of the subchannel. Both RV and IV remains 60 % of lateral velocity during developed Z/D_h= 1 to Z/D_h=3, by the measured lateral area where the maximum lateral velocity observed. SV remains 50% of lateral velocity along with developing inside the channel.

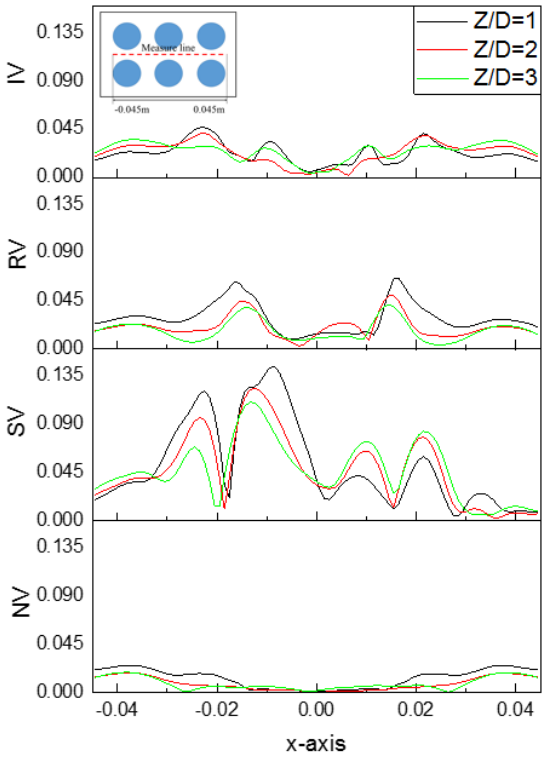

Fig. 3. Lateral velocity distribution along axial position (V_{inlet}=0.5 m/s)

Figure 4 indicates the lateral velocity of the vane types each NV, SV, RV, and IV. NV shows little lateral velocity due to the swirl effect was not observed. Fig. 4 (b), SV shows the most lateral velocity occurred by the vane between other vanes. Flow direction is changed after entering vane structure RV and IV show more lateral velocity than NV, but the averaged magnitude of lateral velocity was smaller than SV.

In contrast, in terms of lateral flow development direction, SV shows flow direction toward x-axis or y-axis along with each split vane. RV and IV implies flow direction to the center of the subchannel, with rotational direction at the center position of the flow channel. Due to the centrifugal force, fluid near the fuel surface would be transferred into the center of the subchannel.

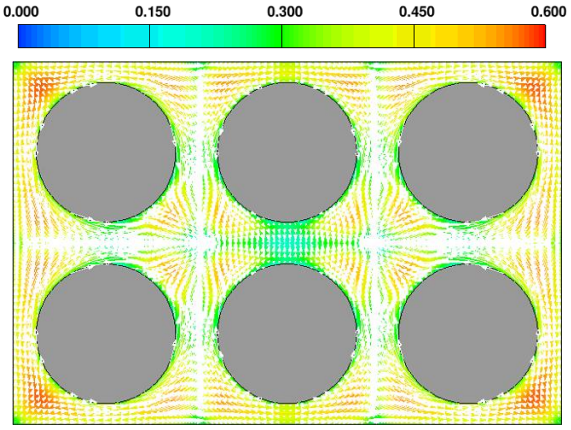

(a) NV

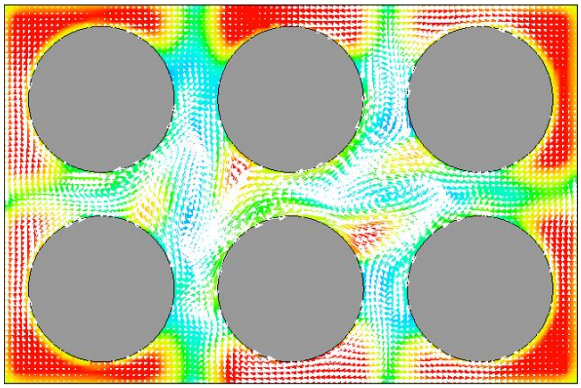

(b) SV

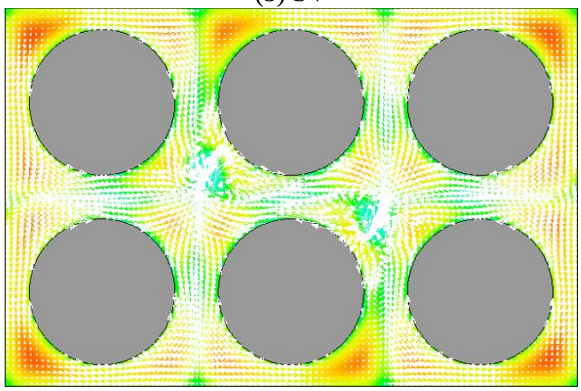

(c) RV

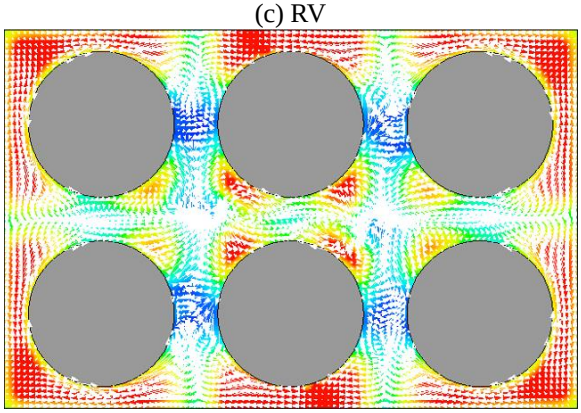

(d) IV

Fig. 4. Velocity magnitude and lateral velocity vector

4. Conclusions

CFD analysis was conducted for the moving rotational vane (RV) and impeller rotational vane (IV), comparing with no vane (NV) and conventional fixed split vane (SV) using commercial code, FLOW-3D. Two types of rotational mixing vanes are investigated in terms of swirl generation and by comparing swirl decay of each type of vane. The swirl performance was evaluated by lateral velocity distribution. Split vane has the best swirling effect with the highest magnitude of lateral velocity in same position with others. In contrast, rotational and impeller vanes, the influenced area from swirl developed is evenly distributed inside the subchannel.

In summary, for rotational and impeller vanes, lateral velocity were not improved compared to maximum lateral velocity of split vane, instead, even swirl effect toward the center of the subchannel were acquired by those vanes.

For the validation of simulation, flow visualization experiment in same geometry with various type of mixing vanes will be performed to evaluate swirl effect by particle image velocimetry (PIV) measurement.

ACKNOWLEDGMENT

This work was supported by the Nuclear Energy Research Program through the National Research Foundation of Korea (NRF), funded by the Ministry of Science and ICT(MSIT) (2017R1A2B2008031, NRF-22A20153413555, 2016M2A8A6900481,).

REFERENCE

[1] H. Seo, S. D. Park, S. B. Seo, H. Heo, I. C. Bang, Swirling performance of low-driven rotating mixing vane toward critical heat flux enhancement, International Journal of Heat and Mass Transfer, vol. 89, p. 1016-1229, 2015.

[2] M. E. Conner, E. Baglietto, A. M. Elmahdi, CFD methodology and validation for single-phase flow in PWR fuel assemblies, Nuclear Engineering and Design, vol. 240, p 2088-2095, 2010.

[3] I. C. Bang, S. H. Chang, Flow mixing rotation vane attached in nuclear fuel spacer, Korea Patent, No. 10-0456500, 2004.

[4] S. K. Chang, S. K Moon, W. P. Back, Y. D. Choi, Phenomenological investigations on the turbulent flow structures in a rod bundle array with mixing devices, Nuclear Engineering and Design, vol. 238, p.600-609, 2008.

[5] Flow science, flow-3D user Manual Version 3.2, 2009.

[6] Y. Lixin, Z. Megnjun, T. Zihao, Heat transfer enhancement with mixing vane spacers using the field synergy principle, Chinese journal of mechanical engineering, vol. 30, No. 1, 2016.